UDK 548/549:549.67
Original scientific article/Izvirni znanstveni članek

ISSN 1580-2949
Mater. Tehnol.

HYDROTHERMAL SYNTHESIS AND CHARACTERIZATION OF ZSM-5 ZEOLITE FROM ANORTHOSITE: IMPACTS OF REACTION TIME AND TEMPERATURE

HIDROTERMALNA SINTEZA IN KARAKTERIZACIJA ZSM-5 ZEOLITA IZ ANORTOZITA: VPLIV REAKCIJSKEGA ČASA IN TEMPERATURE

Yonas Desta Bizualem[1], Mudasir Akbar Shah[2], Soumaya Ibrahimi[3], Aicha Gasmi[3], Noureddine Elboughdiri[4,5]*

[1]Department of Chemical Engineering, Kombolcha Institute of Technology, Wollo University, P.O. Box: 208, Kombolcha, Ethiopia
[2]Department of Chemical Engineering, King Fahd University of Petroleum and Minerals, Dhahran 31261, Saudi Arabia
[3]Department of Chemical Engineering, Laboratory of Engineering Processes and Industrial Systems, National School of Engineering of Gabes, University of Gabes, 6029 Gabes, Tunisia
[4]Chemical Engineering Department, College of Engineering, University of Ha'il, P.O. Box 2440, Ha'il 81441, Saudi Arabia
[5]Chemical Engineering Process Department, National School of Engineers Gabes, University of Gabes, Gabes 6029, Tunisia

Prejem rokopisa – received: 2024-08-23; sprejem za objavo – accepted for publication: 2024-12-02

doi:10.17222/mit.2024.1283

Anorthosite was used as the alumina source while applying a hydrothermal method for the synthesis of ZSM-5. The anorthosite sample, obtained from the Soji-Bikilal region of Ethiopia, was pre-treated and activated with NaOH at a 1:2 (wt/wt) ratio. ZSM-5 type zeolites were made from the anorthosite rock utilising hydrothermal synthesis at reaction times of (24, 48, and 96) h at a reaction temperature of 100 °C, in accordance with the alkaline fusion technique. UV-vis spectra, X-ray diffraction, scanning electron microscopy and BET surface area were used to characterize anorthosite and synthesized ZSM-5 zeolite. The highest noticeable reflection peak for the ZSM-5 zeolite synthesised at the reaction temperature of 100 °C and reaction time of 96 h was at 24.7°, showing that the material was extremely crystalline. According to their microstructures, anorthosite features platy crystals and amorphous particles, while ZSM-5 zeolite exhibits spherical crystals with some amorphous gel.

Keywords: anorthosite, zeolite, hydrothermal synthesis, ZSM-5

Avtorji v članku opisujejo raziskavo uporabe anortozita za hidrotermalni postopek sinteze ZSM-5 (Ca-Na alumo-silikat). Vzorce anortozitne skalovine so dobili na področju Soji-Bikilal v Etiopiji in ga za sintezo uporabili kot vir aluminija. Pred sintezo so ga tudi obdelali in aktivirali z NaOH v masnem razmerju 1:2. Zeolite tipa ZSM-5 so avtorji izdelali iz skalovitega anortozitnega nahajališča z uporabo hidrotermalne sinteze pri 100 °C in reakcijskih časih (24, 48 in 96) ur v pogojih alkalne fuzijske tehnike. Za karakterizacijo anortozita in sintetiziranih ZSM-5 zeolitov so uporabili spektroskopijo v ultravijolični in vidni svetlobi (angl.: UV-vis spectra), rentgensko difrakcijo (angl.: X-ray diffraction) in vrstično elektronsko mikroskopijo (SEM; angl.: scanning electron microscopy). Z BET metodo so določili tudi njihov specifični površinski presek delcev (BET; angl.: Brunauer, Emmett and Teller surface area method). Najvišji opažen vrh ("pik") odboja pri 24,7° so avtorji opazili za popolnoma kristaliničen ZSM-5 zeolite, sintetiziran pri 100 °C in trajanju reakcije 96 ur. Karakterizacija anortozita in ZSM-5 zeolitov je pokazala njihovo sestavo v obliki ploščičastih kristalov, amorfnih delcev, kristalov v obliki kroglic, in nekaj amorfnega gela.

Ključne besede: anortozit, zeolit, hidrotermalna sinteza, ZSM-5

1 INTRODUCTION

Zeolites exhibits a three-dimensional tetrahedral framework structure, consisting of aluminosilicates with AlO_4 and SiO_4 compounds. Molecularly sized holes within the crystal confer various characteristics, such as molecular sieving,[1] cation exchangeability,[2,3] adsorption, and catalysis.[4] These materials attract substantial commercial attention owing to their distinctive pore dimensions reflecting high-value chemical dynamics.[5] Specifically, ZSM-5 zeolites have garnered significant research focus for their exceptional ability to selectively convert chemicals in various industrial applications.[6,7] Zeolites find extensive applications in environmental clean-up, biotechnological applications, pharmaceutical uses, catalytic activity and gas sensing.[8,9] Though naturally occurring zeolites are widely accessible, the current emphasis is on synthetic zeolites because of their ease of production in a pure form, superior ion exchange capacities, and consistent size. ZSM-5 is one of the synthetic zeolites.[10] In the context of the methanol-to-hydrocarbons (MTH) reaction, ZSM-5 zeolites consistently exhibit elevated selectivity towards light aromatics, like xylene-BTX, toluene, and benzene.[11–13] This process stands out as a significant innovation in the ongoing exploration of zeolites and processes related to heterogeneous catalysis.[13] Traditional ZSM-5 zeolites exhibit a considerable grain size at the micrometer level. This

*Corresponding author's e-mail:
ghilaninouri@yahoo.fr (Noureddine Elboughdiri)

characteristic unavoidably prolongs the residence time of products and macromolecular intermediates within the inter-channel space.[14] Consequently, the narrow pores of these zeolites are susceptible to rapid blockage due to coke deposition, resulting in a prompt deactivation of zeolite catalysts.

Numerous techniques have been employed to augment the diffusion properties and improve the catalyst performance of ZSM-5 zeolites. These methods include the preparation of hierarchical ZSM-5[15–17] structures and the utilization of nano-sized ZSM-5 configurations.[18–21] The catalytic efficiency of hierarchical ZSM-5 is notably elevated due to the favorable attributes of both mesoporous materials and microporous zeolites. Regarding hierarchical ZSM-5 zeolites, the micropores within these structures demonstrate exceptional shape selectivity toward the intended main yields. Moreover, the inclusion of mesopores offers benefits in facilitating the transfer of macromolecules, resulting in a noteworthy enhancement of the coke-handling capability of these zeolites. In ZSM-5 with nano-sized particles, a diminished micro size signifies a shorter internal diffusion path, facilitating a swift transmission of large macromolecular yields within a short timeframe.

Consequently, the deactivation of the catalyst due to pore blockage slows down, leading to a significant extension in the catalyst lifetime for these zeolites.

Numerous techniques have been established for zeolite synthesis, including molten salt treatment, hydrothermal treatment, hydrothermal treatment following alkali melting, and hybrid procedures.[22–25] The hydrothermal approach is extensively employed in zeolite synthesis due to its simplicity, scalability, and low energy requirements.[10,26] ZSM-5 is predominantly produced through hydrothermal synthesis utilizing an organic cation template from an alkaline silicate-aluminate mother liquid. Its exceptional thermal and acid stability, high selectivity, and activity in catalytic transformations, especially in shape-selective catalysis, make ZSM-5 indispensable for industrial applications. It is widely utilized as a catalyst in the petrochemical sector for isomerization, alkylation, and aromatization processes, resulting in substantial demand.[27] The synthesis of zeolite during a hydrothermal process is influenced by factors such as alkalinity, pressure, temperature, ageing process, and the development of crystallization nuclei.[28] In this study, the hydrothermal technique was employed to manufacture ZSM-5 zeolite from anorthosite rock, a natural aluminum silicate. The resulting material underwent comprehensive chemical and physical characterization.

1.1 Anorthosite rock

Anorthosite, a rock comprising over 90 % plagioclase, a highly aluminum-rich and acid-soluble silicate mineral, is prevalent in the basement rocks of Norway and Greenland.[29] The chemical formula for anorthosite mineral is $CaAl_2Si_2O_8$. Proterozoic features massif-type anorthosite magmatic rocks.[30] Lunar anorthosite, a significant rock in the lunar highlands, forms through plagioclase floatation in the lunar magma ocean (LMO), shedding light on the early magmatic origin of terrestrial planets. Separating plagioclase with a low crystal percentage from the magma ocean is crucial for generating pure lunar anorthosite, as crystal networks impede synthesis when magma's crystal percentage exceeds 40–60 φ/%.[31] Shallow magma systems in major igneous provinces and mid-ocean ridges contain plagioclase-rich cumulates, reflecting three eras of the original lunar

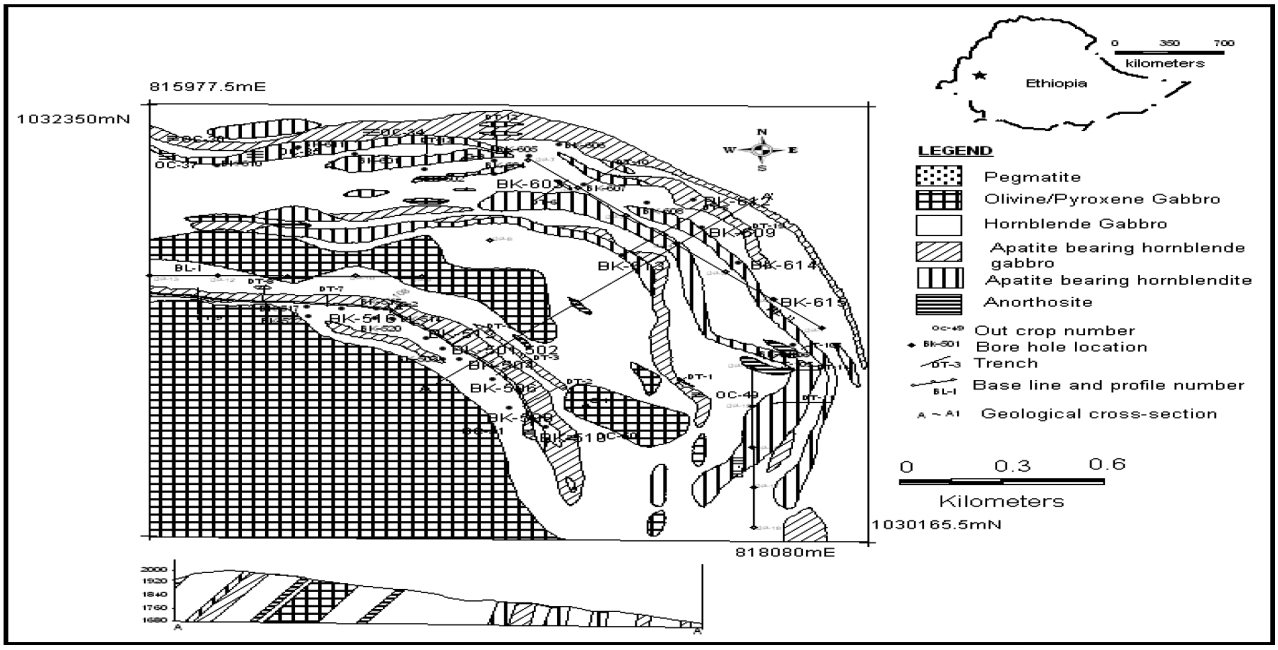

Figure 1: Geology and mineralization map of Soji-Bikilal, Ethiopia: location of anorthosite rock[33]

crust: primordial, Archean megacrystic, and Proterozoic massif-type anorthosite.[32] Investigating natural shear zones in the anorthositic Marcy massif in the Adirondack Mountains of New York, Hodge (2019) aimed to address knowledge gaps.[33] The Marcy anorthosite, located in the Adirondack Highlands, represents the southernmost point of the Grenville Province on Canada's east coast.[33] In the Soji-Bikila region, Western Ethiopia, the primary lithological units include olivine gabbro, hornblende gabbro and hornblendite, and anorthosite. The geology and mineralogy map of anorthosite in the Soji-Bikila region, Western Ethiopia, is illustrated in **Figure 1**.

Recent scientific efforts have focused on utilizing natural minerals to synthesize zeolites, expanding beyond traditional raw materials like kaolin, andalusite, kyanite, sillimanite, and fly ash. Zeolites can now be derived from diverse sources with a high silicon-to-aluminum ratio,[35] offering economic advantages compared to synthetic substrates.[36] ZSM-5, a prominent zeolite, functions as a catalyst for hydrocarbon catalytic cracking due to its distinctive pore structure, acidity, and admirable thermal and hydrothermal firmness.[34,37,38]

2 MATERIALS AND METHODS

All materials utilized in the preparation of zeolites were of analytical reagent grade. High-purity sodium hydroxide (NaOH) was employed as the activating agent for a raw anorthosite rock, serving the dual purpose of activation and pH adjustment during the gel formation process. Concurrently, pH adjustment was achieved using analytical-grade sulfuric acid until the gel formation was realized. Anorthosite sourced from the Bikilal-Ghimbi region in Western Ethiopia was utilized as the precursor source for the preparation of ZSM-5 zeolite. Distillate was employed for the preparation of slurry and cleaning of the crystal zeolite.

During the agitation procedure for dissolving Si and Al salts, a hot plate served as the heat source. The synthesized zeolite underwent drying in an electric oven. The activation of the raw anorthosite and sodium hydroxide mixture was achieved using an electric furnace (Nabertherm L-154K1LN1B1, Germany), and pH levels during gel formation were monitored using a pH meter (Thermo Fisher Scientific, Thermo Scientific Orion Star, A111 Benchtop, USA). A centrifugal separator facilitated the separation of the transparent solution post-gel formation and hydrothermal processing. Crystalline zeolite production utilized a digital autoclave (Digital Autoclave Lx-B 35L, Labdex, UK). Subsequent to the zeolite synthesis, description procedures, including X-ray diffraction (Bruker D8-Advance, USA), scanning electron microscopy (JEOL JSM-6390 LV, USA), BET surface area analyzer (BET-X3000, Labdex Ltd, UK), and UV-2400 PC spectroscopy (UV-2400 PC Spectrophotometer, Labdex, UK), with a diffuse reflectance accessory, were applied. The instrumentation utilized for characterizations was accessible at Addis Ababa University of Science and Technology, Ethiopia.

2.1 Anorthosite collection and preparation

To produce ZSM-5 zeolite, the raw material was obtained from an anorthosite rock located in the Soji-Bikilal region of Western Ethiopia, approximately 405 kilometers from Addis Ababa. Anorthosite was subjected to air drying at room temperature, followed by initial crushing using a crusher and subsequent sieving with a 75 μm pore size.

To activate the raw anorthosite, a mixture of NaOH and anorthosite powder was prepared at a weight ratio of 1:2 (wt/wt). Specifically, 20 g of anorthosite powder and 24 g of NaOH were combined in a crucible, and the resulting mixture was subjected to activation in a furnace. The activation method involved heating the crucible to a temperature of 450 °C for a period of 12 h. Subsequently, 800 g of anorthosite were immersed in 1.5 liters of water, adhering to a solid-to-liquid ratio of 1/1.9 g/mL, to form slurry. This slurry was allowed to soak for 24 h to facilitate dissolution of impurities and undesirable components. After soaking, the slurry underwent sieving with a mesh size of 350 μm, followed by drying after decanting the top surface water. To ensure the exclusion of particles larger than 100 μm, the resulting dry cake was ground and sieved according to the techniques revealed by Mgbemere et al. (2018).[39]

The resultant powder, derived from the activated anorthosite-NaOH reaction, was dissolved in distilled water with a solid-to-liquid ratio of 1/4.9 g/mL of the fused product. During this phase, the slurry underwent heating on a magnetic stirrer hot plate, with vigorous stirring at a temperature of 100 °C for varying reaction times of (24, 48, 96) h.[40] Upon agitation and subsequent filtration, a clear solution was obtained. By reducing the pH of the filtered solution below 10 through the addition of H_2SO_4 while stirring, a white amorphous gel was formed. Subsequently, the newly formed gel was transferred to a sample container for hydrothermal processing. Hydrothermal treatment was conducted in an autoclave, where the gel aged for 2 h before being placed in a 443 K oven for an additional 72 h. The final product underwent multiple centrifugation cycles to achieve a neutral pH, followed by drying at 373 K for 12 h. The resulting material was then finely ground into a powder and sieved to a particle size of 75 μm for subsequent analyses.

2.2 Anorthosite and zeolite characterization

The textural properties of both anorthosite and synthesized ZSM-5 zeolite were evaluated through N_2 adsorption using a Micromeritics TriStar device at 77 K. Prior to analysis, the samples underwent vacuum degassing and were dried at 473 K for 2 hours. X-ray powder diffraction patterns, recorded in a 2θ range of 5° to 70° with Cu Kα radiation at a scanning rate of 2 °/min, were

employed to identify the crystalline structures of anorthosite and synthesized ZSM-5 zeolite.[39] Scanning electron spectroscopy (SEM) was utilized to examine the morphology of the materials, with a thin gold coating applied to enhance conductivity. Morphological details were further elucidated by combining energy-dispersive X-ray (EDX) mapping with SEM for both anorthosite and synthesized ZSM-5 zeolite samples. Furthermore, the chemical characteristics of synthesized ZSM-5 zeolite and anorthosite were investigated using UV-vis spectroscopy.

3 RESULTS AND DISCUSSION

3.1 Anorthosite and ZSM-5 zeolite textural description

Textural features of anorthosite and synthesized ZSM-5 zeolite samples were determined through nitrogen adsorption measurements at 77 K. The obtained surface characteristics, encompassing BET surface area (SBET), total pore volume (Vp), and average pore diameter (d_{ave}), are documented in **Table 1**. Anorthosite exhibited the smallest surface area among the synthesized materials, indicating lower pore abundance of its structure. This observation is significant as it provides insights into the porosity of anorthosite, with potential implications for its performance across diverse applications. Conversely, ZSM-5, a zeolite synthesized over 96 h, demonstrated the highest surface area, specifically 150 g/m^2. This outcome suggests a direct correlation between the surface area and reaction time, implying that prolonged reactions lead to larger surface areas. A plausible explanation for this phenomenon is the generation of additional pores during the gel formation and subsequent hydrothermal treatment processes. This underscores a direct impact of synthesis duration on the porous structure of the material. The gel formation and hydrothermal treatment processes are believed to contribute to the creation of extra pores, thereby augmenting the surface area.

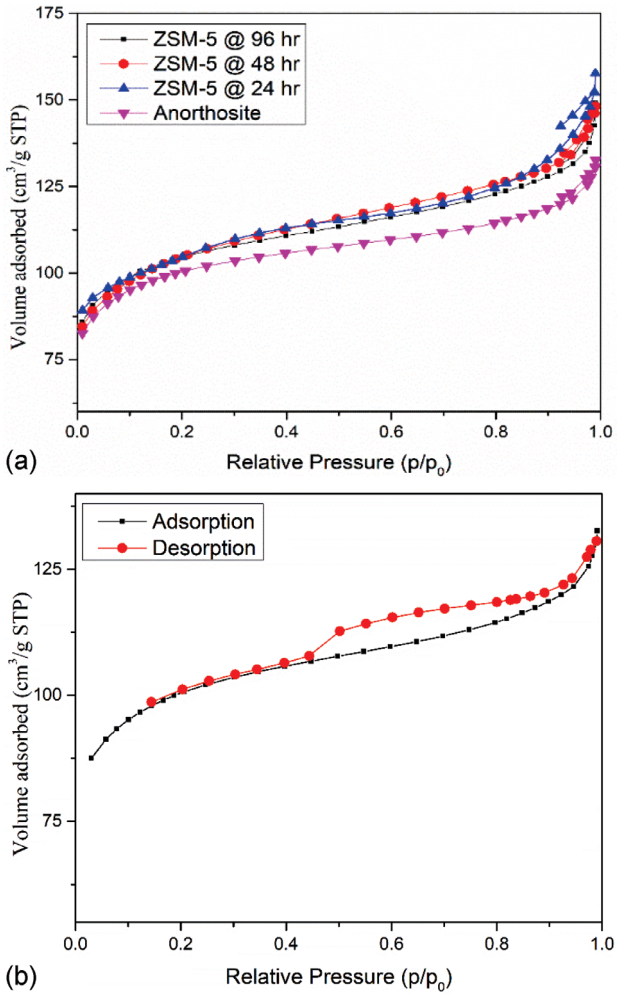

Figure 2: a) Nitrogen adsorption isotherms for anorthosite and ZSM-5 zeolite synthesized over reaction times of (24, 48 and 96) h, and at a reaction temperature of 100 °C, b) isotherms depicting the adsorption and desorption of N_2 for ZSM-5 zeolite, generated at a reaction temperature of 100 °C and over a reaction time of 96 h

Understanding the relationship between synthesis conditions and material properties is pivotal for tailoring materials with specific characteristics for diverse applications. The enhanced surface area of ZSM-5 synthesized over 96 h is advantageous in applications requiring high surface area and porosity, such as catalysis or adsorption processes. A study by Smail et al. (2019) produced a similarly uniform mesoporous zeolite ZSM-5 catalyst with surface areas, pore diameters, and volumes comparable to those from the present investigation.[41] Additionally, the surface area result aligns with the findings by Yang et al. (2020), who explored the impact of hydrochloric acid-treated HZSM-5 zeolite.[41] In comparison, Yang et al. (2020) observed that the addition of hydrochloric acid (HCl) increased the specific surface area (175.0 to 300.4 m^2/g) of HZSM-5 zeolite, expanding both microporous and mesoporous materials. However, this expansion reached a limit as the concentration of HCl increased.[42]

Table 1: Surface characterizations of anorthosite rock and hydrothermally synthesized ZSM-5 zeolite at various temperatures

Sample type	S_A (m^2/g)	V_P (cm^3/g)	D_{ave} (nm)
Anorthosite	40.8	0.112	2.600
ZSM-5 for 24 h	120.2	0.134	2.488
ZSM-5 for 48 h	132.8	0.1986	2.479
ZSM-5 for 96 h	150.4	0.2420	2.320

Nitrogen adsorption and adsorption-desorption isotherms of ZSM-5 zeolites, synthesized at different reaction durations (24, 48, and 96 h) under a constant reaction temperature of 100 °C, are depicted in **Figures 2a** and **2b**. The isotherms across all samples exhibit characteristics typical of mesoporous materials. This distinction is significant as it offers insights into the inherent porous structure of the produced ZSM-5 zeolites. The mesopores and adsorption mechanism are likely outcomes of

the synthesis, caused, particularly, by the reaction time and temperature. The protracted reaction times may contribute to the generation of additional pores, thereby influencing the mesoporous nature of zeolite.[43]

3.2 X-ray diffraction and SEM investigation of anorthosite and ZSM-5 zeolite

The X-ray diffraction curves of anorthosite and ZSM-5 zeolite synthesized over various reaction times (24, 48, and 96 h) at a constant reaction temperature of 100 °C are presented in **Figure 3**. The anorthosite pattern exhibits a notable presence of impurities, particularly quartz, evidenced by low-intensity peaks at 2θ = 8–10° and 2θ = 24–30°. Mullite, forming a chemically stable glassy surface layer atop quartz, contributed to a highly intense peak. Despite the discernible quartz peak in the anorthosite raw material curve, the presence of amorphous material is observed. Upon anorthosite treatment, sharp and highly intense diffraction peaks emerge, indicative of the zeolite formation. Concurrently, certain mullite and quartz peaks diminish, while new peaks appear. The XRD patterns of ZSM-5 produced from anorthosite and obtained with hydrothermal processing, display more distinct peaks. **Figure 2** demonstrates that, except for anorthosite, all samples display characteristic diffraction peaks at (2θ = 7.2°, 8.4°, 15.6°, 21.7°, 24.8°, 30.1°, and 45.1°), consistent with the zeolite structure. In alignment with our findings, Guo et al. (2011) investigated the synthesis and characterization of hierarchical ZSM-5 zeolites using hydrothermal techniques and organosilanes as additives. Their study revealed typical diffraction peaks at 2θ of 24.40°, 23.90°, 23.18°, 14.78°, 8.80° and 7.92° mirroring the observations in our current investigation.[44]

This outcome aligns with the findings from a prior investigation conducted by Wang P. et al. (2007), wherein ZSM-5 zeolite was produced from anorthosite.[27] The XRD patterns reveal that the ZSM-5 zeolite, subjected to a 96-h reaction time, exhibits the most prominent peak, followed by the 48-hour sample, while the 24-hour response time yields the lowest peak intensity. This trend suggests that the reaction time during the gel formation exerts a discernible influence on crystal development, as evidenced by the XRD pattern. Furthermore, a direct correlation is observed between the synthetic zeolite's crystal size and peak intensity. In general, the findings of this study indicate a substantial transformation of anorthosite into high-purity ZSM-5 zeolite. However, residual quartz from the raw material persists in the synthesized materials. The increased crystallite dimensions of the zeolite are attributed to a higher presence of pores and voids, as the structural periodicity of zeolites inherently promotes these characteristics.[45,46]

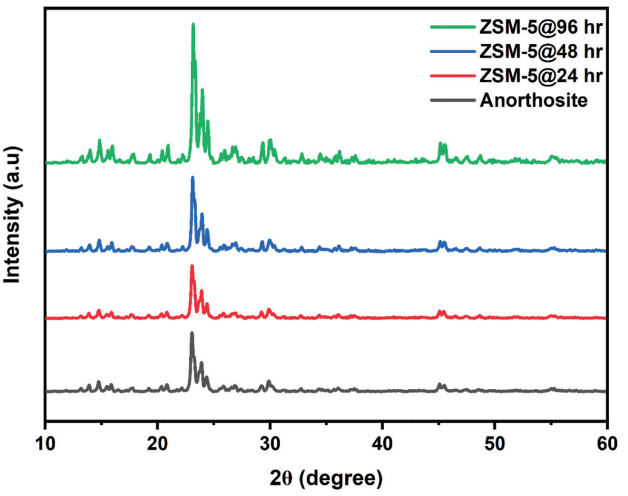

Figure 3: XRD curves of anorthosite and ZSM-5 zeolite synthesized over (24, 48, and 96) h at a reaction temperature of 100 °C

Scanning electron microscopy (SEM) was employed to thoroughly investigate the morphological characteristics of both anorthosite and ZSM-5 zeolite under different experimental conditions. Samples were collected at intervals of (24, 48, and 96) h, all treated at a consistent reaction temperature of 100 °C, as depicted in **Figure 4**. Remarkably, anorthosite exhibits no observable crystal features, suggesting that its structural attributes may not be readily discernible under the specified reaction conditions. However, a notable transformation is noted after a 24 h reaction period, characterized by attempts to induce the formation of a foam-like structure. Subsequently, with an extension of the reaction period to 48 h, there is a distinct shift as spherically shaped crystals begin to emerge. The present study aligns with the findings of Anuwattana et al. (2008) on the synthesis of a uniform mesoporous zeolite ZSM-5 catalyst for Friedel-Crafts acylation.[47]

The temporal evolution in morphology becomes more pronounced over the 96 hr period, when the ZSM-5 crystal exhibits well-defined and fully developed spherical shapes. This outcome align with the observations made by Sanhueza et al. (2004) during the synthesis of ZSM-5 from diatomite.[11] Sanhueza et al. (2004) observed spherical and cubic shapes after 20 h at 150 °C, suggesting a correlation between the response time (96 h) and the detection of spherical shapes in the current study using a lower temperature. The greatest crystallinity of ZSM-5 was observed after 24 h, indicating that 150 °C for 24 hours was the optimal temperature for the ZSM-5 synthesis. Similar results were reported by Anuwattana et al. (2008), regarding the hydrothermal formation of zeolite ZSM-5 from cupola slag, carried out both conventionally and via microwaving.[47] This report on morphological transitions underscores the dynamic impact of reaction time on the structural development of ZSM-5 zeolite, providing valuable insights into the kinetics and mechanisms governing its synthesis. In addition to facilitating a detailed observation of these intricate morphological changes, SEM also positioned itself as an indispensable tool for unraveling the complex in-

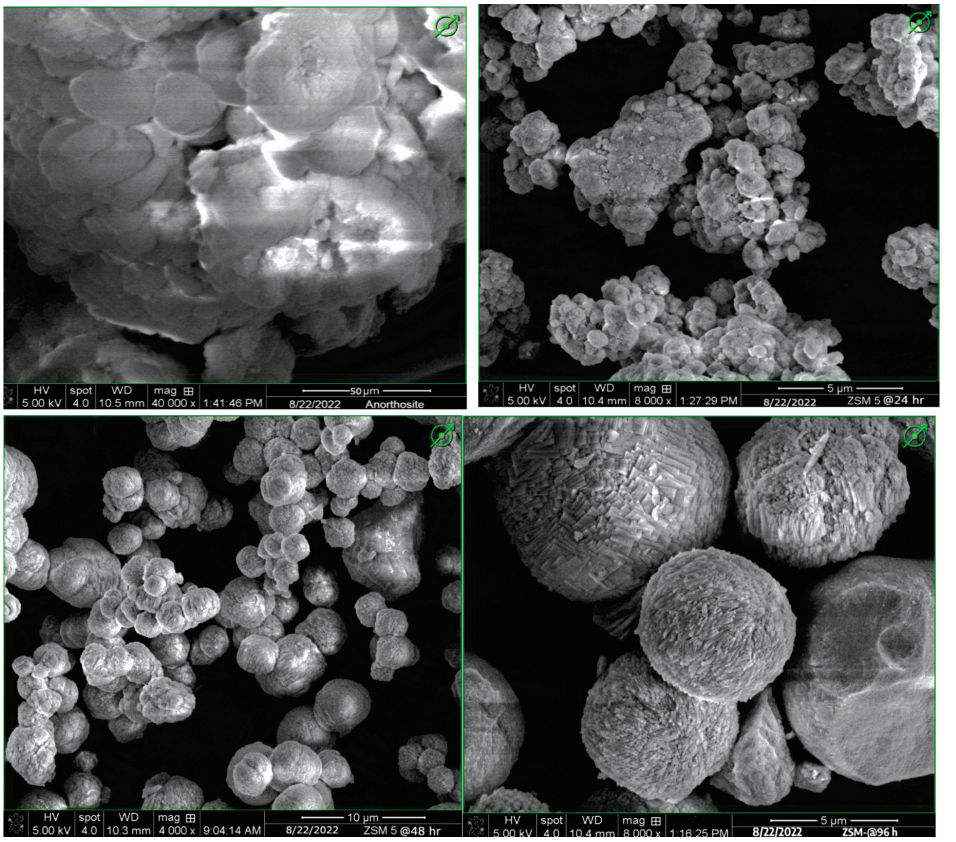

Figure 4: SEM figures of: a) anorthosite and ZSM-5 zeolite obtained at the reaction temperature of 100 °C and reaction times of b) at 24 h, c) at 48 h, d) at 96 h

terplay of factors shaping a material's evolution over time.[27]

3.3 UV-vis spectra of anorthosite and ZSM-5 zeolite

The UV-vis spectra of anorthosite and synthetic ZSM-5 obtained over reaction times of (24, 48, and 96) h, and at a reaction temperature of 100 °C, are presented in **Figure 5**. The shape and intensity of the spectra during gel formation are observed to be notably dependent on the reaction time. Unlike anorthosite and ZSM-5 zeolite synthesized over 24 h, the spectra of ZSM-5 zeolites synthesized over 48 and 96 h exhibit a prominent absorption band in a range of 190–390 nm. Additionally, a significant UV-vis absorption band emerges between 190 nm and 290 nm for anorthosite and ZSM-5 zeolite obtained over 24 h. This implies that as the reaction time increases during the gel formation, both the intensity and the bandwidth of the absorption bands extend towards longer wavelengths.

Interestingly, anorthosite and ZSM-5 zeolite synthesized over the 24-h reaction period exhibit a broadened shape of the spectra, accompanied by an increased absorbance tail at longer wavelengths, as seen in the **Figure 5**. This broadening can be attributed to the presence of amorphous and impure constituents within anorthosite. It is noteworthy that during the hydrothermal synthesis of ZSM-5 zeolites, those formed over longer reaction times tend to exhibit higher intensity compared to those formed over shorter reaction times. Further insights into the sub-bands and nuances of UV-vis spectra analysis for various forms of ZSM-5 can be found in recent research papers.[48,49] These studies delve deeper into the spectral characteristics and provide a more compre-

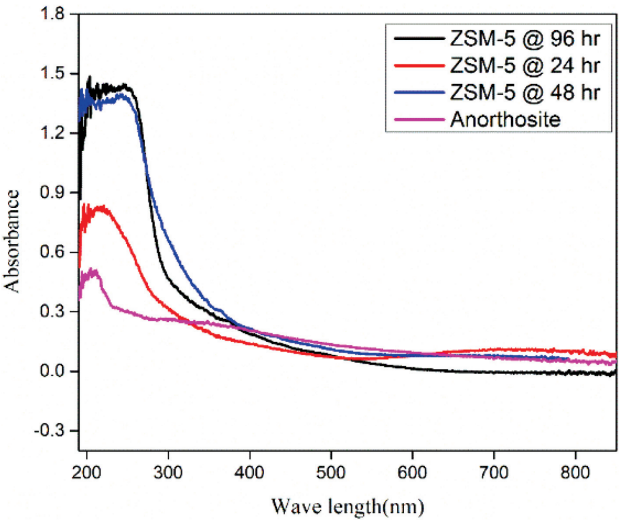

Figure 5: UV-Vis spectra of anorthosite and ZSM-5 zeolite obtained over reaction times of 24, 48 h and 96 h and at a reaction temperature of 100 °C

hensive understanding of the structural and compositional variations observed in ZSM-5 zeolite.

The presence of low-intensity bands in the UV-vis spectra suggests the existence of impurity phases, such as amorphous silica, in the synthesized ZSM-5 zeolite, underscoring the importance of a thorough spectral analysis in material characterization. Overall, the UV-vis spectra analysis of anorthosite and ZSM-5 zeolite provided valuable information about their structural integrity, purity, and potential applications in various fields such as catalysis, adsorption, and environmental remediation. Further studies combining UV-vis spectroscopy with other analytical techniques could provide deeper insights into the molecular-level properties and behavior of these materials, facilitating their optimization for specific technological applications.

4 CONCLUSION

In conclusion, the hydrothermal activation of anorthosite using NaOH has demonstrated its viability as an effective precursor for synthesizing high-purity ZSM-5 zeolite. The results highlight the significant role of anorthosite and its chemical composition in the transformation process. Notably, ZSM-5 synthesized over different reaction times (24, 48, and 96) h and at a constant temperature of 100 °C exhibited distinct improvements in crystallinity and purity, evidenced by sharper diffraction peaks compared to the raw anorthosite. The optimal synthesis conditions, specifically the period of 96 h, yielded a ZSM-5 zeolite with a surface area of 150.4 m²/g, indicating enhanced material properties suitable for various applications. X-ray diffraction (XRD) revealed the evolution of the crystalline structure, transitioning from an amorphous composition to well-defined zeolite peaks, while UV-vis spectroscopy identified the presence of impurities such as amorphous silica. Furthermore, scanning electron microscopy (SEM) confirmed the formation of well-defined ZSM-5 crystals, contrasting the amorphous nature of anorthosite. These findings underscore the potential of utilizing anorthosite as a sustainable and effective source for zeolite synthesis, opening avenues for further research into optimizing conditions for enhanced material properties and exploring its applications in catalysis and environmental remediation.

Acknowledgement

The authors would like to acknowledge the Department of Chemical Engineering at Kombolcha Institute of Technology, Wollo University, Ethiopia, and the Department of Chemical Engineering at King Fahd University of Petroleum & Minerals, Dhahran 31261, KSA, for their valuable assistance and conducive environment that facilitated the completion of this paper.

Author contribution

Yonas Desta Bizualem: Writing original draft preparation, Conceptualization, Methodology, Investigation validation, Data curation. *Mudasir Akbar Shah*: Draft preparation, Investigation validation, Data curation, Reviewing and editing. *Soumaya Ibrahimi*: Reviewing and editing, Conceptualization, Methodology, Data curation. *Aicha Gasmi*: Reviewing and editing, Methodology, Investigation validation, Data curation. *Noureddine Elboughdiri*: Writing original draft preparation, Reviewing and editing, Conceptualization, Methodology, Investigation validation, Data curation.

Data availability statement

All research data can be found within this publication.

Conflict of interest

The authors declare no conflicting, contending, or financial interests in any capacity.

Declaration of generative AI in scientific writing

The authors affirm that they did not employ generative AI in the creation of the manuscript at any stage.

5 REFERENCE

[1] S. Wang, Y. Duan, Y. Wei, L. Xu, J. Li, Tuning the siting of aluminum in ZSM-11 zeolite and regulating its catalytic performance in the conversion of methanol to olefins, J. Catal., 377 (**2019**), 81–97

[2] A. Rujiwatra, A selective preparation of phillipsite and sodalite from perlite, Mater. Lett., 58 (**2004**) 14, 2012–2015

[3] M. Boronat, A. Corma, What is measured when measuring acidity in zeolites with probe molecules?, ACS Catal., 9 (**2019**) 2, 1539–1548

[4] D. J. Kim, H. S. Chung, Synthesis and characterization of ZSM-5 zeolite from serpentine, Appl. Clay Sci., 24 (**2003**) 1–2, 69–77

[5] D. Serrano, J. Aguado, J. M. Escola, J. M. Rodríguez, Molecular and meso- and macroscopic properties of hierarchical nanocrystalline ZSM-5 zeolite prepared by seed silanization, Chem. Mater., 21 (**2009**) 4, 641–654

[6] Y. T. Cheng, J. Jae, J. Shi, W. Fan, G. W. Huber, Production of p-xylene from biomass by catalytic fast pyrolysis using ZSM-5 catalysts with reduced pore openings, Angew. Chem., 124 (**2012**) 44, 11259–11262

[7] A. Chawla, N. Kumari, S. Kumar, Cooperative effects of inorganic and organic structure-directing agents in ZSM-5 crystallization, Mol. Syst. Des. Eng., 3 (**2018**) 1, 159–170

[8] A. Corma, State of the art and future challenges of zeolites as catalysts, J. Catal., 216 (**2003**) 1–2, 298–312

[9] N. Elboughdiri, The use of natural zeolite to remove heavy metals Cu(II), Pb(II) and Cd(II) from industrial wastewater, Cogent Engineering, 7 (**2020**), 1782623, doi:10.1080/23311916.2020.1782623

[10] A. Khaleque, S. S. Alam, S. Maghsoudi, Zeolite synthesis from low-cost materials and environmental applications: A review, Environ. Adv., 2 (**2020**), 100019

[11] V. Sanhueza, U. Kelm, A. López, Synthesis of ZSM-5 from diatomite: a case of zeolite synthesis from a natural material, J. Chem. Technol. Biotechnol., 79 (**2004**) 7, 686–690

[12] E. N. Coker, S. Li, A. J. Bolton, Zeolite ZSM-5 synthesized in space: catalysts with reduced external surface activity, Microporous Mesoporous Mater., 46 (**2001**) 2–3, 223–236

[13] J. García-Martínez, M. Johnson, J. Valla, Synthesis and characterization of MFI-type zeolites supported on carbon materials, Microporous Mesoporous Mater., 42 (**2001**) 2–3, 255–268

[14] H. Zhang, Y. Li, H. Wang, Nano-crystallite oriented self-assembled ZSM-5 zeolite and its LDPE cracking properties: Effects of accessibility and strength of acid sites, J. Catal., 302 (**2013**), 115–125

[15] J. Ding, L. Zhu, X. Li, Catalytic properties of a hierarchical zeolite synthesized from a natural aluminosilicate mineral without the use of a secondary mesoscale template, ChemCatChem, 5 (**2013**) 8, 2258–2269

[16] Z. Xue, S. Yang, X. Chen, Hierarchical structure and catalytic properties of a microspherical zeolite with intracrystalline mesopores, Acta Mater., 60 (**2012**) 16, 5712–5722

[17] M. Moliner, C. Martínez, A. Corma, Multipore zeolites: synthesis and catalytic applications, *Angew.* Chem. Int. Ed., 54 (**2015**) 12, 3560–3579

[18] M. Firoozi, M. Baghalha, M. Asadi, The effect of micro and nano particle sizes of H-ZSM-5 on the selectivity of MTP reaction, Catal. Commun., 10 (**2009**) 12, 1582–1585

[19] M. Choi, H. S. Cho, R. Srivastava, Stable single-unit-cell nanosheets of zeolite MFI as active and long-lived catalysts, Nature, 461 (**2009**) 7261, 246–249

[20] A. A. Rownaghi, J. Hedlund, Methanol to gasoline-range hydrocarbons: influence of nanocrystal size and mesoporosity on catalytic performance and product distribution of ZSM-5, Ind. Eng. Chem. Res., 50 (**2011**) 21, 11872–11878

[21] H. Konno, Y. Sasaki, I. Nakamura, Effectiveness of nano-scale ZSM-5 zeolite and its deactivation mechanism on catalytic cracking of representative hydrocarbons of naphtha, Microporous Mesoporous Mater., 175 (**2013**), 25–33

[22] M. Wdowin, W. Franus, R. Panek, The conversion technology of fly ash into zeolites, Clean Technol. Environ. Policy, 16 (**2014**), 1217–1223

[23] M. Park, H. Katsuki, Y. Oumi, Molten-salt method for the synthesis of zeolitic materials: I. Zeolite formation in alkaline molten-salt system, Microporous Mesoporous Mater., 37 (**2000**) 1–2, 81–89

[24] F. Mondragon, A. Molina, J. Garcia, New perspectives for coal ash utilization: synthesis of zeolitic materials, Fuel, 69 (**1990**) 2, 263–266

[25] K. Ojha, N. C. Pradhan, A. N. Samanta, Zeolite from fly ash: synthesis and characterization, Bull. Mater. Sci., 27 (**2004**), 555–564

[26] J. L. X. Hong, B. Xu, L. Liu, Conversion of coal fly ash into zeolite materials: synthesis and characterizations, process design, and its cost-benefit analysis, Ind. Eng. Chem. Res., 56 (**2017**) 40, 11565–11574

[27] P. Wang, B. Shen, J. Gao, Synthesis of ZSM-5 zeolite from expanded perlite and its catalytic performance in FCC gasoline aromatization, Catal. Today, 125 (**2007**) 3–4, 155–162

[28] R. V. de la Villa Mencia, R. M. Moreno, S. M. Garcia, Synthesis of zeolite type analcime from industrial wastes, Microporous Mesoporous Mater., 293 (**2020**), 109817

[29] C. Knudsen, J. Wanvik, H. Svahnberg, Anorthosites in Greenland: a possible raw material for aluminium?, GEUS Bull., 26 (**2012**), 53–56

[30] A. E. Osmanlioglu, Immobilization of radioactive waste by cementation with purified kaolin clay, Waste Management, 22 (**2002**) 5, 481–483

[31] T. Arai, S. Maruyama, Formation of anorthosite on the Moon through magma ocean fractional crystallization, Geoscience Frontiers, 8 (**2017**) 2, 299–308

[32] L. D. Ashwal, G. M. Bybee, Crustal evolution and the temporality of anorthosites, Earth-Science Reviews, 173 (**2017**), 307–330

[33] W. Mammo Ghebre, Geology and Mineralization of Bikilal phosphate deposit, Western Ethiopia, implication and outline of gabbro intrusion to East Africa zone, Iranian Journal of Earth Sciences, 2 (**2010**), 158–167

[34] B. W. Woldemichael, J.-I. Kimura, Petrogenesis of the Neoproterozoic Bikilal-Ghimbi gabbro, Western Ethiopia, J. Mineral. Petrol. Sci., 103 (**2008**) 1, 23–46

[35] Y. He, et al., Research progress on green synthesis of various high-purity zeolites from natural material-kaolin, J. Clean. Prod., 306 (**2021**), 127248

[36] M. Król, Natural vs. synthetic zeolites, Crystals, 10 (**2020**) 7, 622

[37] T. Blasco, A. Corma, J. Martínez-Triguero, Hydrothermal stabilization of ZSM-5 catalytic-cracking additives by phosphorus addition, J. Catal., 237 (**2006**) 2, 267–277

[38] N. Xue, et al., Synergistic effects of tungsten and phosphorus on catalytic cracking of butene to propene over HZSM-5, Appl. Catal. A-Gen., 352 (**2009**) 1–2, 87–94

[39] H. Mgbemere et al., Synthesis of zeolite-A using kaolin samples from Darazo, Bauchi state, and Ajebo, Ogun state in Nigeria, Niger. J. Technol., 37 (**2018**) 1, 87–95

[40] C. A. Ríos, C. D. Williams, O. M. Castellanos, Crystallization of low silica Na-A and Na-X zeolites from transformation of kaolin and obsidian by alkaline fusion, Ing. Competitividad, 14 (**2012**) 2, 125–137

[41] H. A. Smail, et al., Synthesis of uniform mesoporous zeolite ZSM-5 catalyst for Friedel-Crafts acylation, ChemEngineering, 3 (**2019**) 2, 35

[42] L. Yang, et al., Role of hydrochloric acid treated HZSM-5 zeolite in $Sm_2Ti_2O_7$/nHZSM-5 composite for photocatalytic degradation of ofloxacin, J. Mater. Res. Technol., 9 (**2020**) 5, 10585–10596

[43] B. K. Singh, et al., Synthesis of mesoporous zeolites and their opportunities in heterogeneous catalysis, Catalysts, 11 (**2021**) 12, 1541

[44] Y.-P. Guo, et al., Fabrication and characterization of hierarchical ZSM-5 zeolites by using organosilanes as additives, Chem. Eng. J., 166 (**2011**) 1, 391–400

[45] M. S. Hamdy, F. A. Alqahtani, M. Shkir, K. F. Fawy, M. Benaissa, M. B. B. Hamida, N. Elboughdiri, Effect of different zeolite supports on the catalytic behavior of platinum nanoparticles in cyclohexene hydrogenation reaction, Catalysts, 12 (**2022**), 1106, doi:10.3390/catal12101106

[46] P. Klobes, R. G. Munro, Porosity and specific surface area measurements for solid materials, 2006

[47] R. Anuwattana, et al., Conventional and microwave hydrothermal synthesis of zeolite ZSM-5 from the cupola slag, Microporous Mesoporous Mater., 111 (**2008**) 1–3, 260–266

[48] M. S. Kumar, et al., On the nature of different iron sites and their catalytic role in Fe-ZSM-5 DeNOx catalysts: New insights by a combined EPR and UV/VIS spectroscopic approach, J. Catal., 227 (**2004**) 2, 384–397

[49] M. Schwidder, et al., Selective reduction of NO with Fe-ZSM-5 catalysts of low Fe content: I. Relations between active site structure and catalytic performance, J. Catal., 231 (**2005**) 2, 314–330